The Canadian Mineralogist
Vol. 37, pp. 199-206 (1999)

COORDINATION AND LOCAL STRUCTURE OF MAGNESIUM IN SILICATE MINERALS AND GLASSES: Mg *K*-EDGE XANES STUDY

DIEN LI[1]

College of Earth and Environment Sciences, Zhongshan University, Guangzhou, Guangdong 510275, People's Republic of China, and Earth and Environment Sciences Division, MS D469, Los Alamos National Laboratory, Los Alamos, New Mexico 87545, U.S.A.

MINGSHENG PENG

College of Earth and Environment Sciences, Zhongshan University, Guangzhou, Guangdong 510275, People's Republic of China

TAKATOSHI MURATA

Department of Physics, Kyoto University of Education, Kyoto 612, Japan

Abstract

We present Mg *K*-edge XANES spectra of selected Mg-bearing oxide and silicate minerals with different coordination states of Mg. The Mg *K*-edge peak shifts to higher energy with increasing coordination, from $^{[4]}$Mg in spinel, to $^{[5]}$Mg in grandidierite, to $^{[6]}$Mg in diopside and many other silicates, and to $^{[8]}$Mg in pyrope. The correlation between the energy of the Mg *K*-edge and Mg–O bond distance of the model minerals is also established; it can be used to estimate the average Mg–O bond distance in disordered systems. The curve fitting of Mg *K*-edge XANES spectra may be used to distinguish the coordination of Mg, and to determine the relative proportion of different coordination sites, as demonstrated in yoderite, which contains both $^{[5]}$Mg and $^{[6]}$Mg. The structural role of Mg in $CaMgSi_2O_6$ (Di) – $NaAlSi_3O_8$ (Ab) glasses was studied using Mg *K*-edge XANES spectra. The Mg–O bond distance in these glasses is estimated to be 2.00 ± 0.04 Å. Thus, Mg in these glasses may be five-coordinated with oxygen, or Mg may have multiple structural sites, $^{[4]}$Mg, $^{[5]}$Mg and $^{[6]}$Mg. Structurally, the Di–Ab glasses may possess a medium-range order, and have dramatically different multiple scattering (MS) paths from those of crystalline model minerals.

Keywords: Mg *K*-edge XANES, silicate minerals, $CaMgSi_2O_3$ – $NaAlSi_3O_8$ glasses, coordination of Mg.

Sommaire

Nous présentons ici des résultats de la spectroscopie d'absorption X au seuil *K* (XANES) du magnésium dans une sélection d'oxydes et de silicates porteurs de Mg dans des coordinences diverses. Le pic du seuil *K* est décalé vers une énergie plus élevée à mesure qu'augmente la coordinence, de $^{[4]}$Mg dans le spinelle à $^{[5]}$Mg dans la grandidierite, à $^{[6]}$Mg dans le diopside et plusieurs autres silicates, et finalement à $^{[8]}$Mg dans le pyrope. La corrélation entre l'énergie associée au seuil *K* et la longueur de la liaison Mg–O dans les minéraux choisis est aussi établie; on peut s'en servir pour prédire le longueur moyenne de la liaison Mg–O dans les systèmes désordonnés. La courbe simulant le spectre du seuil *K* du Mg peut servir à distinguer la coordinence du Mg, et à déterminer la proportion relative des sites à coordinence différente, comme dans la yoderite, qui contient à la fois $^{[5]}$Mg et $^{[6]}$Mg. Le role structural du Mg dans des verres dont la composition est située entre $CaMgSi_2O_6$ (Di) et $NaAlSi_3O_8$ (Ab) a été étudié avec cette approche spectroscopique. La liaison Mg–O dans ces verres aurait une longueur de 2.00 ± 0.04 Å. C'est donc dire que dans ces verres, le Mg pourrait bien montrer une coordinence cinq avec l'oxygène, ou bien il pourrait occuper plus d'un site, $^{[4]}$Mg, $^{[5]}$Mg et $^{[6]}$Mg. Du point de vue structural, ces verres Di–Ab pourraient posséder une mise en ordre à moyenne échelle, et avoir des dispersions multiples de rayons X différant de façon marquée des structures cristallines des minéraux modèles.

(Traduit par la Rédaction)

Mots-clés: seuil *K* du Mg, XANES, minéraux silicatés, verres $CaMgSi_2O_3$ – $NaAlSi_3O_8$, coordinence du Mg.

[1] *E-mail address*: dienli@lanl.gov

Introduction

Magnesium is dominantly six-coordinated ($^{[6]}$Mg) with oxygen in oxide and silicate minerals (Smyth & Bish 1988). However, Mg has also been found to be four-coordinated ($^{[4]}$Mg) in spinel, magnesiochromite and åkermanite (Yang *et al.* 1997), five-coordinated ($^{[5]}$Mg) in grandidierite (Stephenson & Moore 1968) and yoderite (Higgins *et al.* 1982), and eight-coordinated ($^{[8]}$Mg) with oxygen in pyrope. Mg-bearing silicate phases are believed to be the major components of the lower mantle. Mg is also a major constituent in most primitive and undifferentiated magmas. The structure and coordination of Mg in silicate melts are deemed important in understanding the dynamic and physical properties of silicate magmas, such as element partitioning, and transport properties including viscosity and diffusion. The coordination and local structure of Mg in silicate minerals and glasses have been studied using X-ray emission, vibrational spectroscopy (Kubicki *et al.* 1992, McMillan 1984, McMillan *et al.* 1992), ^{25}Mg magic angle spinning (MAS) NMR (MacKenzie & Meinhold 1994a, b, Stebbins 1996), Mg *K*-edge X-ray absorption near-edge structure (XANES), and molecular dynamic simulation (Matsui & Price 1991, Matsui 1996), as well as X-ray diffraction (Smyth & Bish 1988) and X-ray scattering (Yin *et al.* 1983, Okuno & Marumo 1993). In most of these studies, the authors concluded that Mg may be accommodated in distorted sites, but the coordination geometry of Mg in silicate glasses and melts remains very controversial (Brown *et al.* 1995). We use Mg *K*-edge XANES spectroscopy further to study the coordination and local structure of some model silicate minerals and glasses; this approach is deemed to provide important insight into the structure of silicate melts.

Background Information

Among the applications of Mg *K*-edge XANES spectroscopy to geological materials, Ildefonse *et al.* (1995) reported Mg *K*-edge spectra of model crystalline compounds such as spinel, periclase and pyrope; Mottana *et al.* (1995) briefly compared experimental data with calculations at the Mg *K*-edge of diopside and omphacite. More recently, Wu *et al.* (1996) and Cabaret *et al.* (1998) carried out full multiple scattering (FMS) calculations at the Mg *K*-edge of olivine (forsterite) and pyroxenes (diopside and enstatite). These FMS calculations provided excellent simulation of the experimental Mg *K*-edge XANES spectra of these minerals.

However, the relationship of Mg *K*-edge XANES spectroscopy to the coordination and local structure (*e.g.*, Mg–O bond distance, the bond valence of Mg with oxygen, the distortion of the Mg–O polyhedron) involving Mg in Mg-bearing oxides and silicates is not well established and understood. Mg *K*-edge XANES spectroscopy has been rarely applied to a study of the coordination and local structure of disordered Mg-bearing systems (*e.g.*, silicate glasses and melts). In this work, experimental Mg *K*-edge XANES spectra of selected Mg-bearing oxide and silicates with different coordination geometries are presented. The relationship of Mg *K*-edge spectra to the coordination and local structure of Mg is established. Mg *K*-edge XANES spectroscopy has also been used to a study of the coordination and local structure of Mg in $CaMgSi_2O_6$ (Di) – $NaAlSi_3O_8$ (Ab) glasses, and proven to be useful as a structural fingerprint to provide important information for Mg in other disordered systems.

Experimental

Samples

Samples of Mg-bearing oxide and silicate minerals were obtained primarily from the Department of Earth Sciences, University of Western Ontario, and Department of Mineralogy, Royal Ontario Museum. The samples were characterized by optical petrography and powder X-ray diffraction (PXRD), and found to be single phases. The chemical formula and some of the structural parameters are summarized in Table 1. The $CaMgSi_2O_6$ (Di) – $NaAlSi_3O_8$ (Ab) glasses are taken from the study of Keppler (1992). Mixtures of glassy powders of albite and diopside starting materials were melted in a platinum crucible using a room-pressure high-temperature gas-mixing furnace. Experiments were performed in air. After usually 12–24 hours at 1200–1500°C, samples were quenched by dropping the crucible into cold water. Other details on the sample preparation and composition of these glasses are given in Keppler (1992).

TABLE 1. CHEMICAL COMPOSITION AND STRUCTURE PARAMETERS OF MODEL OXIDES AND SILICATES

Minerals	Formula	CN	d_{Mg-O} (Å)	s_{Mg-O}
Pyrope	$Mg_3Al_2Si_3O_{12}$	8	2.270	1.682
Montmorillonite	$Na_{0.38}(Al,Mg)_2Si_4O_{10}(OH)_2{\cdot}nH_2O$	6		
Lizardite	$Mg_3Si_{1.83}Al_{0.17}O_5(OH)_4$	6	2.066	2.190
Talc	$Mg_3Si_4O_{10}(OH)_2$	6	2.071	2.160
Diopside	$CaMgSi_2O_6$	6	2.077	2.125
Enstatite	$MgSiO_3$	6	2.115	1.930
Cordierite	$Mg_2Si_5Al_4O_{18}$	6	2.110	1.944
Forsterite	Mg_2SiO_4	6	2.111	1.938
Grandidierite	$(Mg,Fe)Al_3SiBO_9$	5	2.042	1.947
Spinel	$MgAl_2O_4$	4	1.924	2.143
Yoderite	$^{[6]}(MgAl_3)^{[5]}(MgAl)^{[5]}(Al_{0.84}Fe_{0.16})_2O_2(SiO_4)_3(OH)_2$	5 6	1.933 1.963	2.641 2.892

CN: Coordination number of Mg; d_{Mg-O}: Mg–O bond distance; s_{Mg-O}: bond valence of Mg with O. The data on CN and d_{Mg-O} are compiled from Smyth & Bish (1988), except for grandidierite (Stephenson & Moore 1968) and yoderite (Higgins *et al.* 1982); s_{Mg-O} is calculated from the formula given by Brown & Altermatt (1985). The data are averaged if there are multiple Mg sites (*e.g.*, forsterite, enstatite and talc). The chemical formula of montmorillonite is cited from Powell *et al.* (1997).

Mg K-edge measurements

Mg *K*-edge XANES spectra were measured using the BL–7A beamline at UVSOR in the Institute for Molecular Sciences, Japan. The beamline used beryl (d_{100} = 7.9825 Å) as the monochromator crystal. The storage ring was operated at an energy of 750 MeV and a current of 80–190 mA. The samples were ground into fine powder and mounted on a copper sample cell, and the sample holder was transferred into the chamber, where pressure is below 10^{-6} torr. Mg *K*-edge XANES spectra were collected in one scan using the total-electron-yield mode at room temperature. The interval of data points is 0.2 eV in the near-edge region. A linear background was removed for each spectrum, but the spectra shown were not smoothed. The energy calibration was made using the Mg *K*-edge peak of MgO at 1311.3 eV. The Mg *K*-edge XANES spectra were decomposed into Gaussian components by fitting in order to obtain the energy position and relative intensity of each peak in the Mg *K*-edge XANES spectra. In each of the fitting procedures, an Arctan edge background was applied, the linewidths of peaks above 1320 eV were constrained, but the energy position and amplitude of all peaks are fitted, assuming that the line shape of each peak is of Gaussian type. The residue between the experimental spectrum and the spectral envelope from fitting is small, indicating that the quality of the fittings is acceptable.

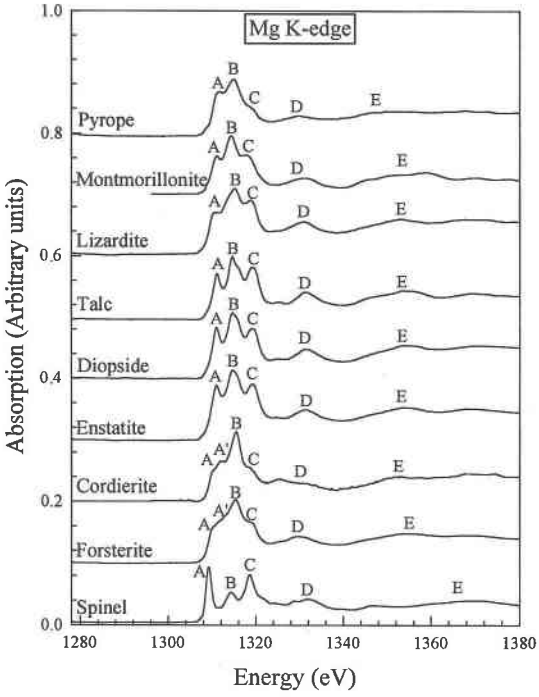

FIG. 1. Mg *K*-edge XANES spectra of Mg-bearing model mineral samples at the energy range of 1290–1380 eV: pyrope ($^{[8]}$Mg), montmorillonite ($^{[6]}$Mg), lizardite ($^{[6]}$Mg), talc ($^{[6]}$Mg), diopside ($^{[6]}$Mg), enstatite ($^{[6]}$Mg), cordierite ($^{[6]}$Mg), forsterite ($^{[6]}$Mg) and spinel ($^{[4]}$Mg).

RESULTS AND DISCUSSION

Interpretation of Mg K-edge spectra

Figure 1 shows the Mg *K*-edge XANES spectra of spinel, forsterite, cordierite, enstatite, diopside, talc, lizardite, montmorillonite and pyrope in the energy range from 1290 to 1380 eV. The energy position and relative intensity of each peak are summarized in Table 2. Whether Mg is eight- (as in pyrope), or six- (as in diopside) or four-coordinated (as in spinel) with oxygen in these model minerals, the Mg *K*-edge XANES spectra have some features in common: there are three prominent features at the near-edge energy region from 1308 to 1324 eV, labeled as A, B and C; there are two or three broad oscillations at the post-edge energy range from 1324 up to 1380 eV, labeled as D and E. There is also a weak, but discernible pre-edge peak before peak A. However, for forsterite and cordierite, there is another peak between peaks A and B, which is labeled as A'.

The interpretation of the near-edge features in X-ray absorption spectra is still very controversial. The classic explanation is based on molecular orbital theory, in which the edge peak, for example, peak A in Mg *K*-edge spectra, is due to the electronic transition from 1*s* to an empty bound 3*p*-like state (Yoshida *et al.* 1995). A more thoroughly tested interpretation over the last decade involves multiple scattering (MS) theory. Thus, in MS theory, the Mg *K*-edge spectra are divided into two regions: a full multiple-scattering (FMS) region

TABLE 2. ENERGY POSITION AND RELATIVE INTENSITY OF Mg *K*-EDGE XANES OF OXIDES AND SILICATES

Minerals	Position (±0.1 eV)					Intensity		
	A	A'	B	C	E	A	B	C
Pyrope	1311.7		1314.8	1318.4	1345.8	0.1155	0.1910	0.0683
Montmorillonite	1310.9		1314.3	1318.1	1356.4	0.1062	0.2531	0.1861
Lizardite	1311.0		1314.7	1318.9	1353.2	0.1054	0.2962	0.1817
Talc	1311.1		1314.8	1319.1	1354.5	0.1027	0.2000	0.2246
Diopside	1311.1		1314.9	1319.0	1354.4	0.1044	0.2169	0.1650
Enstatite	1311.2		1314.7	1318.9	1354.4	0.1688	0.3413	0.3174
Cordierite	1310.4	1312.4	1315.3	1318.7	1351.7	0.0163	0.0779	0.0297
Forsterite	1310.3	1312.6	1315.3	1318.7	1353.3	0.1943	0.5093	0.3545
Grandidierite	1310.9	1313.7	1315.8	1318.8		0.0277	0.0177	0.0300
Spinel	1309.2		1314.3	1318.9	1365.6	0.1033	0.0677	0.1688
Yoderite								
$^{[5]}$Mg	1310.2	1312.4	1315.0	1319.7		0.0389	0.0363	0.0440
$^{[6]}$Mg	1310.8		1314.2	1317.9		0.0286	0.0555	0.0440

covers the energy range up to 15 eV above the edge peak A at about 1310.0 eV, and the prominent features arise from the contribution of many MS paths; an intermediate multiple scattering (IMS) region covers the energy range from the FMS region up to 1380 eV, where a few weak features arise from a small number of MS paths of lower order.

It is very difficult to properly interpret the Mg *K*-edge spectra of the model minerals without detailed FMS calculations for each structure-type with differing MS paths, which is not attempted in this work. However, Wu *et al.* (1996) and Cabaret *et al.* (1998) have carried out quantitative FMS calculations at the Mg *K*-edge of olivine (forsterite) and pyroxene (diopside and enstatite), respectively, and provided excellent simulations of the experimental Mg *K*-edge spectra of these geological materials. These FMS calculations provide a basis for the qualitative interpretation of the current experimental Mg *K*-edge spectra of other model samples. Peaks B and E are related to the first coordination shell, peak B may be attributed to the electronic transition of 1*s* to the empty bound 3*p*-like state within the first coordination sphere (Wu *et al.* 1996), and peak E is assigned to the shape resonance of the first Mg–O coordination shell (Cabaret *et al.* 1998). Peaks A, C and D are related to the multiple scattering from the outermost coordination shells around the absorbing Mg, as shown by the fact that peaks A and C in the Mg *K*-edge spectra of diopside and enstatite were nicely reproduced when the 7.3 Å cluster was included in the FMS calculation (Cabaret *et al.* 1998). Peak A' in the Mg *K*-edge spectra of forsterite and cordierite may be related to the very strong distortion of the first Mg–O coordination shell (see Table 1) resulting in significantly different MS paths from the more outer shells, in agreement with the calculated *K*-edge spectrum of Mg in the *M*2 site in enstatite (Cabaret *et al.* 1998). The Mg *K*-edge spectrum of spinel is very distinct, because of tetrahedrally coordinated Mg. However, the more accurate assignment of peaks and full explanation of the Mg *K*-edge spectra of spinel and the other silicate minerals are very difficult because no theoretical calculations were attempted in this work.

Mg K-edge spectra versus coordination and local structure

Figure 2 shows Gaussian peak fits to the Mg *K*-edge XANES spectra of pyrope ($^{[8]}$Mg), diopside ($^{[6]}$Mg), grandidierite ($^{[5]}$Mg), and spinel ($^{[4]}$Mg) in the energy range of 1300–1340 eV. The energy position and relative intensity of each peak are summarized in Table 2. As coordination changes from four to eight in these model minerals, peak A shifts to higher energy, becomes broader, and its amplitude tends to decrease. Peak B remains at a relatively constant energy, but the relative amplitude tends to increase even though its linewidth remains similar; peak C in the pyrope spectrum is relatively weak. In addition, another peak, A', has been observed between peaks A and B in the grandidierite spectrum. The post-edge features tend to become richer and more complicated with the change from pyrope, through diopside and grandidierite, to spinel.

Yoderite, $^{[6]}(MgAl_3)^{[5]}(MgAl)^{[5]}(Al_{0.84}Fe_{0.16})_2O_2(OH)_2(SiO_4)_4$, contains both $^{[6]}$Mg and $^{[5]}$Mg in a 1:1 ratio in the *A*1 and *A*2 sites, respectively (Higgins *et al.* 1982). The Mg *K*-edge XANES spectrum of yoderite is shown in Figure 3a. We used the spectrum of a montmorillonite as a model to decompose the Mg *K*-edge spectrum of yoderite, because Mg and Al form isomorphous substitution in the octahedron layer of a montmorillonite, and the Mg:Al atomic ratio in the *M* sites of a montmorillonite is reasonably similar to that (1:3) of Mg over Al in the *A*1 site of yoderite. Since the atomic ratio of $^{[6]}$Mg in the *A*1 site over $^{[5]}$Mg in the *A*2 site is 1:1, peak B in the montmorillonite spectrum

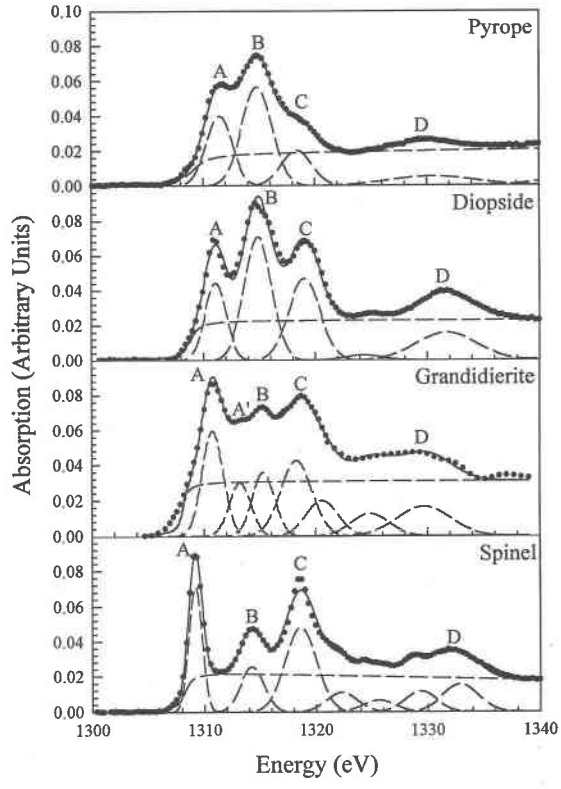

FIG. 2. Mg *K*-edge spectra of pyrope ($^{[8]}$Mg), diopside ($^{[6]}$Mg), grandidierite ($^{[5]}$Mg) and spinel ($^{[4]}$Mg) over the energy range of 1300–1340 eV. The lines of filled circles are the experimental Mg *K*-edge spectra, the dashed lines are the Gaussian components, and the solid lines are the fitted spectra; an Arctan edge background was applied in each of the fitting procedures.

(Fig. 3b) was aligned to the half amplitude of peak B in Mg *K*-edge spectrum of yoderite. Thus, the difference between montmorillonite and yoderite is the Mg *K*-edge spectrum for $^{[5]}$Mg in the *A*2 site of yoderite, which is very similar to the Mg *K*-edge spectrum (see Fig. 2) of grandidierite, which contains $^{[5]}$Mg only (Stephenson & Moore 1968). Therefore, on the basis of curve-fitting and similar reduction of the data, one can use a Mg *K*-edge XANES spectrum to determine the distribution of Mg in different coordination sites of a sample.

Figure 4 shows the correlation between energy of Mg *K*-edge (peak A) and Mg–O bond distance (d_{Mg-O}) of the model minerals. The data for d_{Mg-O} (Å) and energy position (eV) of Mg *K*-edge are summarized in Table 1 and 2, respectively. The correlation is expressed by the equation:

$$y = -27.77\,x^2 + 123.60\,x + 1174.16$$

where y is the energy (eV) of Mg *K*-edge, and x is the d_{Mg-O} (Å). The correlation coefficient is 0.986. Thus, regardless of the exact origins of peak A, this correlation can be used to estimate the Mg–O bond length in Mg-bearing systems in which the structure of Mg is unknown (*e.g.*, silicate glasses and melts, and other amorphous materials). In fact, for $^{[6]}$Mg-bearing silicate minerals only, the Mg *K*- edge (peak A) tends to shift to higher energy with the increase in Mg–O bond distance, but also to shift to lower energy with increase in the bond valence of Mg with oxygen (Fig. 5). The data points of enstatite deviate from the regression lines, possibly because of the presence of two nonequivalent Mg sites, one of which is a very distorted octahedron.

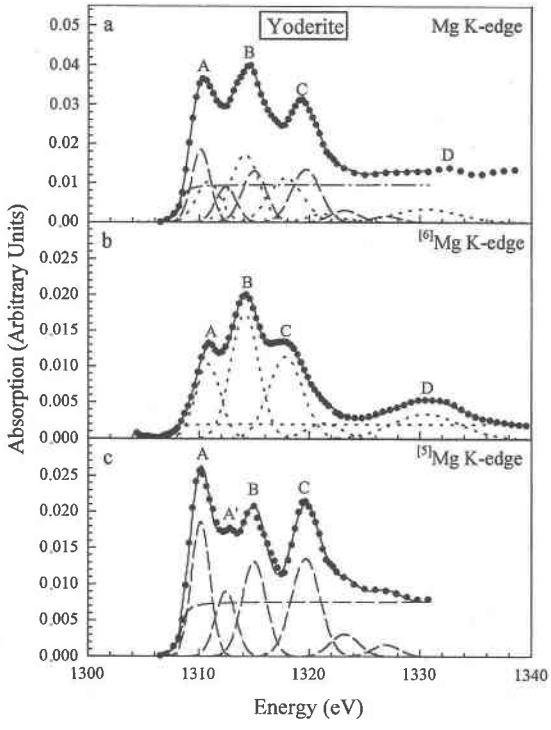

FIG. 3. Mg *K*-edge XANES spectrum (a) of yoderite that contains $^{[6]}$Mg and $^{[5]}$Mg (1:1 ratio). The Mg *K*-edge spectrum of yoderite is decomposed into the spectra for $^{[6]}$Mg (b) and $^{[5]}$Mg (c), by aligning the amplitude of peak B at a 1:1 ratio. The lines of filled circles are experimental spectra, and the dotted lines for $^{[6]}$Mg and dashed lines for $^{[5]}$Mg are the Gaussian components, and the solid lines are the fitted spectra; an arctan edge background was applied in each of the fitting procedures.

Structure role of Mg in $CaMgSi_2O_6$ (Di) – $NaAlSi_3O_8$ (Ab) glasses

Mg *K*-edge XANES spectra can distinguish different coordination geometries of Mg; one may thus apply this approach to study the coordination structure of Mg in disordered systems (*e.g.*, silicate glasses and melts, and amorphous materials). Figure 6 shows Mg *K*-edge XANES spectra of glasses prepared on the join $CaMgSi_2O_6$ (Di) – $NaAlSi_3O_8$ (Ab). The nominal composition, the energy position and relative intensity of Mg *K*-edge spectra of these glasses are summarized in Table 3. Compared with the Mg *K*-edge spectrum of diopside (Fig. 2), the main near-edge peaks (A, B and C) in the Mg *K*-edge spectra of these glasses become broad, and peaks A and C become less prominent and sharp, and the post-edge features above 1320 eV are essentially smeared out. Thus the general profile of the Mg *K*-edge spectra of the Di–Ab glasses is very different from that of diopside. Also as shown in Table 3, the most significant change in the Mg *K*-edge spectra of these glasses is that the Mg *K*- edge (peak A) shifts to

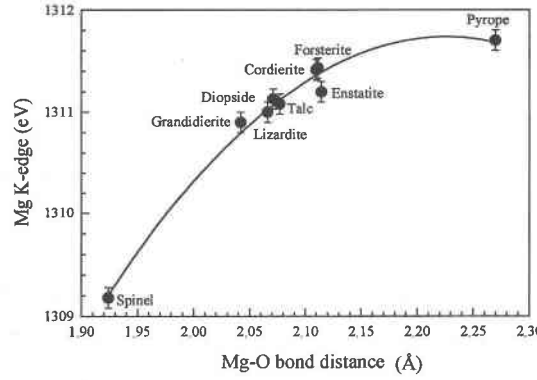

FIG. 4. The correlation between energy position (eV) of peak A in the Mg *K*-edge spectra and Mg–O bond distance (Å) of the model minerals.

TABLE 3. COMPOSITION, ENERGY AND RELATIVE INTENSITY OF Mg *K*-EDGE PEAKS AND ESTIMATED Mg–O BOND DISTANCE (d_{Mg-O}) IN $CaMgSi_2O_6$ (Di) – $NaAlSi_3O_8$ (Ab) GLASSES

No.	Composition	Position (±0.1 eV)			Intensity			d_{Mg-O} (Å)
		A	B	C	A	B	C	
S 58	Di_{100}	1310.2	1314.3	1317.9	0.032	0.061	0.024	1.99 ± 0.04
S 33	$Di_{50}Ab_{50}$	1310.3	1314.5	1318.0	0.015	0.039	0.013	2.00 ± 0.04
S 51	$Di_{20}Ab_{80}$	1310.3	1314.5	1318.0	0.011	0.026	0.011	2.00 ± 0.04
S 59	$Di_{10}Ab_{90}$	1310.5	1314.4	1318.1	0.008	0.021	0.009	2.02 ± 0.04

lower energy by about 0.8 eV, compared with the Mg *K*-edge of diopside, but peak B remains at a similar energy. In addition, the relative intensity of peaks A, B and C in the Mg *K*-edge spectra of the glasses tends to increase with increasing Di content and thus Mg content, as observed for Mg *K*-edge spectra of the crystalline model samples in Table 2. Thus, Mg *K*-edge XANES spectroscopy can at least qualitatively determine the relative content of Mg in a series of samples if the sample preparation and Mg *K*-edge measurements are done under very similar conditions.

On the basis of the Mg *K*-edge energy position of the Di–Ab glasses and the correlation equation established for the model samples, the Mg–O bond distances of the Di–Ab glasses can be estimated (Table 3). The estimated Mg–O bond length of the Di–Ab glasses is 2.00 ± 0.04 Å, intermediate between [4]Mg (1.924 Å) in spinel and [6]Mg (~2.10 Å) in many other silicates (see Table 1). This Mg–O bond distance is also similar to the Mg–O bond distance of [5]Mg (2.042 Å) in grandidierite, although the substitution of Fe for Mg in the cation site of grandidierite makes this value larger than expected. Thus, on the basis of the Mg–O bond distance of the Di–Ab glasses only, it is likely that Mg is five-coordinated in this series of silicate glasses. Peaks A and C, which are attributed to the MS effect, are observed in the Mg *K*-edge spectra of the Di–Ab glasses, but not as prominently as they are in the model minerals, indicating that the Di–Ab glasses possess moderately ordered structures, and the MS paths are different from those in the crystalline diopside. However, the profiles of the glass Mg *K*-edge spectra are, to a great extent, different from that of grandidierite, which also raises the possibility that some percentage of [4]Mg or [6]Mg species may be present in the Di–Ab glasses.

The coordination and local structure of Mg in silicate glasses and melts have been studied by a number of spectroscopic techniques and molecular dynamic simulations. Some results on $MgSiO_3$ and $CaMgSi_2O_6$

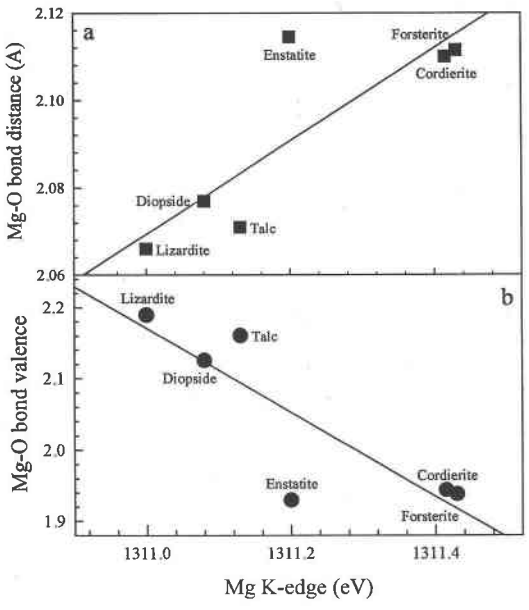

FIG. 5. The correlation of energy position (eV) of peak A in the Mg *K*-edge spectra of [6]Mg-bearing silicate minerals with Mg–O bond distance (a) and calculated bond-valence of Mg with oxygen (b).

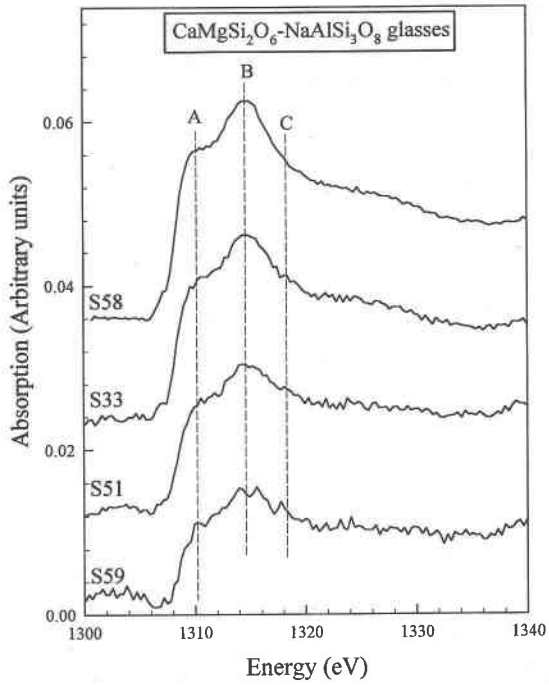

FIG. 6. Mg *K*-edge XANES spectra of glasses prepared along the join $CaMgSi_2O_6$ (Di) – $NaAlSi_3O_8$ (Ab). The nominal composition of each glass sample is shown in Table 3.

TABLE 4. COMPARISON OF STRUCTURAL STUDIES OF Mg^{2+} IN Mg-BEARING SILICATE GLASSES AND MELTS

Materials	Technique	d_{Mg-O} (Å)	Mean CN	Ref.
$MgSiO_3$ glass	X-ray scattering	2.14	4.5	1
$MgSiO_3$ glass	X-ray scattering	2.08	4.1	2
MgO-SiO_2 films	X-ray emission	Not given	4.0	3
$MgSiO_3$ glass	Molecular dynamics	1.9	4.3	4
$Mg_3Al_2Si_3O_{12}$ glass	X-ray scattering	2.10	4.8	5
$(Na_2O)_{0.28}(MgO)_{0.18}(SiO_2)_{0.54}$ liquid	^{25}Mg MAS NMR	2.00 (1400°C)	5	6
$(CaO)_{0.29}(MgO)_{0.14}(SiO_2)_{0.57}$ liquid	^{25}Mg MAS NMR	2.08 (1400°C)	6	6
$CaMgSi_2O_6$ glass	Mg *K*-edge EXAFS	2.01	5	7
$CaMgSi_2O_6$ glass	O *K*-edge EXELFS	1.94	4	8
Di_{100} glass	Mg *K*-edge XANES	1.99	5	9
$Di_{50}Ab_{50}$ glass	Mg *K*-edge XANES	2.00	5	9
$Di_{20}Ab_{80}$ glass	Mg *K*-edge XANES	2.00	5	9
$Di_{10}Ab_{90}$ glass	Mg *K*-edge XANES	2.02	5	9

References: 1: Waseda & Toguri (1977), 2: Yin *et al.* (1983), 3: Hanada *et al.* (1988), 4: Kubicki & Lasaga (1991), 5: Okuno & Marumo (1993), 6: Fiske & Stebbins (1994), 7: Ildefonse *et al.* (1995), 8: Tabira (1996), 9: this study.

glasses and melts are summarized in Table 4, which also shows the mean Mg–O bond distance (d_{Mg-O}) and coordination number (CN) of Mg in $CaMgSi_2O_6$ glasses estimated from Mg *K*- edge XANES spectra. X-ray-scattering studies reveal a mean Mg–O bond distance of 2.14 Å and a mean CN of 4.5 (Waseda & Toguri 1977). However, Yin *et al.* (1983) proposed a mean d_{Mg-O} of 2.08 Å and CN of 4.1, on the basis of fitting their X-ray scattering data to a quasi-crystalline model. X-ray emission and molar reflectivity measurements of sputtered amorphous films in the MgO–SiO_2 system indicated predominantly tetrahedral coordination of Mg where the MgO content is 50% or less (Hanada *et al.* 1988). However, more recent MD simulations suggest a mean Mg–O bond distance of 1.90 Å, corresponding to a mean coordination number for Mg close to 4 (Kubicki & Lasaga 1991). Similarly, a few previous studies are also in conflict with the mean Mg–O bond distance and coordination number of Mg in $CaMgSi_2O_6$ glasses. Fiske & Stebbins (1994) suggested that Mg is six-coordinated with oxygen and the Mg–O bond distance is 2.08 Å in a silicate melt of composition $(CaO)_{0.29}(MgO)_{0.14}(SiO_2)_{0.57}$ at 1400°C, on the basis of ^{25}Mg MAS NMR. However, Ildefonse *et al.* (1995) reported a Mg–O bond distance of 2.01 Å and a coordination number of 5 in a $CaMgSi_2O_6$ glass on the basis of extended X-ray-absorption fine structure (EXAFS) analysis of the Mg *K*-edge. Tabira (1996) indirectly used extended energy-loss fine structure (EXELFS) of the oxygen *K*-edge to investigate the local coordination environment around Mg atoms in a $CaMgSi_2O_6$ glass, and inferred a Mg–O bond length of 1.94 Å and coordination number of 4. As indicated above, we estimated that the Mg–O bond distance is 2.00 ± 0.04 Å and the coordination number of Mg is 5 in $CaMgSi_2O_6$ (Di) – $NaAlSi_3O_8$ (Ab) glasses, on the basis of Mg *K*-edge XANES spectra of these glasses and the correlation between the Mg *K*-edge and Mg–O bond distance for model silicate minerals. However, we are not able to exclude the possibility that there are coexisting $^{[5]}$Mg, $^{[6]}$Mg and $^{[4]}$Mg species in these silicate glasses.

Acknowledgements

We thank M.E. Fleet, Department of Earth Sciences, University of Western Ontario, F.J. Wicks and R. Ramik, Department of Mineralogy, Royal Ontario Museum, Canada, and H. Keppler, Bayerisches Geoinstitut, University of Bayreuth, Germany, for provision of samples. We also appreciate the staff at UVSOR, the Institute for Molecular Sciences, Japan, for their technical assistance, and B. Carey, Los Alamos National Laboratory, for his thorough review of this manuscript. This work was supported by the China Natural Science Foundation (CNSF). DL also thank China International Bridge (CIB) and CNSF for the support of his travel and research work in Zhongshan University, People's Republic of China.

References

Brown, G.E., Farges, F. & Calas, G. (1995): X-ray scattering and X-ray spectroscopy studies of silicate melts. *In* Structure, Dynamics, and Properties of Silicate Melts (J.F. Stebbins, P.F. McMillan & D.B. Dingwell, eds.). *Rev. Mineral.* **32**, 317-340.

Brown, I.D. & Altermatt, D. (1985): Bond-valence parameters obtained from a systematic analysis of the inorganic crystal structure database. *Acta Crystallogr.* **B41**, 244-247.

Cabaret, D., Sainctavit, P., Ildefonse, P. & Flank, A.-M. (1998): Full multiple scattering calculations of the X-ray absorption near edge structure at the magnesium K-edge in pyroxene. *Am. Mineral.* **83**, 300-304.

Fiske, P.S. & Stebbins, J.F. (1994): The structure role of Mg in silicate liquids: a high-temperature ^{25}Mg, ^{23}Na, and ^{29}Si NMR study. *Am. Mineral.* **79**, 848-861.

Hanada, T., Soga, N. & Tachibana, T. (1988): Coordination state of magnesium ions in rf-sputtered amorphous films in the system MgO–SiO_2. *J. Non-Cryst. Solids* **105**, 39-44.

Higgins, J.B., Ribbe, P.H. & Nakajima, Y. (1982): An ordering model for the commensurate antiphase structure of yoderite. *Am. Mineral.* **67**, 76-84.

Ildefonse, P., Calas, G., Flank, A.M. & Lagarde, P. (1995): Low Z elements (Mg, Al, and Si) K-edge x-ray absorption spectroscopy in minerals and disordered systems. *Nucl. Instrum. Methods Phys. Res.* **B97**, 172-175.

Keppler, H. (1992): Crystal field spectra and geochemistry of transition metal ions in silicate melts and glasses. *Am. Mineral.* **77**, 62-75.

KUBICKI, J.D., HEMLEY, R.J. & HOFMEISTER, A.M. (1992): Raman and infrared study of pressure-induced structural changes in $MgSiO_3$, $CaMgSi_2O_6$, and $CaSiO_3$ glasses. *Am. Mineral.* **77**, 258-269.

_____ & LASAGA, A.C. (1991): Molecular dynamics simulations of pressure and temperature effects on $MgSiO_3$ and Mg_2SiO_4 melts and glasses. *Phys. Chem. Minerals* **17**, 661-673.

MACKENZIE, K.J.D. & MEINHOLD, R.H. (1994a): ^{25}Mg nuclear magnetic resonance spectroscopy of minerals and related inorganics: a survey study. *Am. Mineral.* **79**, 250-260.

_____ & _____ (1994b): Thermal reactions of chrysotile revisited: a ^{29}Si and ^{25}Mg MAS NMR study. *Am. Mineral.* **79**, 43-50.

MATSUI, M. (1996): Molecular-dynamics study of the structures and bulk moduli of crystals in the system CaO–MgO–Al_2O_3–SiO_2. *Phys. Chem. Minerals* **23**, 345-353.

_____ & PRICE, G.D. (1991): Simulation of the pre-melting behavior of $MgSiO_3$ perovskite at high pressures and temperatures. *Nature* **351**, 735-737.

MCMILLAN, P. (1984): A Raman spectroscopic study of glasses in the system CaO–MgO–SiO_2. *Am. Mineral.* **69**, 645-659.

_____, WOLF, G. & POE, B.T. (1992): Vibrational spectroscopy of silicate liquids and glasses. *Chem. Geol.* **96**, 351-366.

MOTTANA, A., MURATA, T., WU, ZIYU, MARCELLI, A. & PARIS, E. (1996): Detection of order–disorder in pyroxenes of the jadeite – diopside series via XAS at the Ca–Na and Mg–Al K-edge. *J. Electron Spectros. Related Phenom.* **79**, 79-82.

OKUNO, M. & MARUMO, F. (1993): The structure analyses of pyrope ($Mg_3Al_2Si_3O_{12}$) and grossular ($Ca_3Al_2Si_3O_{12}$) glasses by X-ray diffraction method. *Mineral. J.* **16**, 407-415.

POWELL, D.H., TONGKHAO, K., KENNEDY, S.J. & SLADE, P.G. (1997): A neutron-diffraction study of interlayer water in sodium Wyoming montmorillonite using a novel diffraction method. *Clays Clay Minerals* **45**, 290-294.

SMYTH, J.R. & BISH, D.L. (1988): *Crystal Structure and Cation Sites of the Rock-Forming Minerals*. Allen & Unwin, Boston, Massachusetts.

STEBBINS, J.F. (1996): Magnesium site exchange in forsterite: a direct measurement by high-temperature ^{25}Mg NMR spectroscopy. *Am. Mineral.* **81**, 1315-1320.

STEPHENSON, D.A. & MOORE, P.B. (1968): The crystal structure of grandidierite, $(Mg,Fe)Al_3SiBO_9$. *Acta Crystallogr.* **B24**, 1518-1522.

TABIRA, Y. (1996): Local structure around oxygen atoms in $CaMgSi_2O_6$ glass by O K-edge EXELFS. *Mater. Sci. Eng.* **B41**, 63-66.

WASEDA, Y. & TOGURI, J.M. (1977): The structure of molten binary silicate systems CaO–SiO_2 and MgO–SiO_2. *Metall. Trans.* **8B**, 563-568.

WU, ZIYU, MOTTANA, A., MARCELLI, A., NATOLI, C.R. & PARIS, E. (1996): Theoretical analysis of X- ray absorption near-edge structure in forsterite, Mg_2SiO_4-Pbnm, and fayalite, Fe_2SiO_4-Pbnm, at room temperature and extreme conditions. *Phys. Chem. Minerals* **23**, 193-204.

YANG, HEXIONG, HAZEN, R.M., DOWNS, R.T. & FINGER, L.W. (1997): Structural change associated with the incommensurate-normal phase transition in åkermanite, $Ca_2MgSi_2O_7$, at high pressure. *Phys. Chem. Minerals* **24**, 510-519.

YIN, C.D., OKUNO, M., MORIKAWA, H. & MARUMO, F. (1983): Structure analysis of $MgSiO_3$ glass. *J. Non-Cryst. Solids* **55**, 131-141.

YOSHIDA, T., TANAKA, T., YOSHIDA, H., FUNABIKI, T., YOSHIDA, S. & TAKATOSHI, M. (1995): Study of dehydration of magnesium hydroxide. *J. Phys. Chem.* **99**, 10890-10896.

Received July 29, 1998, revised manuscript accepted December 15, 1998.